

## Supporting Information

### Selective CO<sub>2</sub> adsorption in water-stable alkaline-earth based metal-organic frameworks

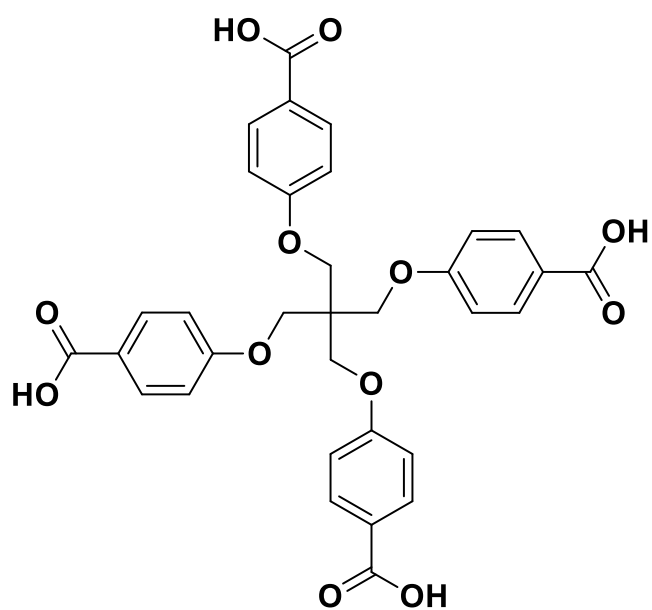
Yiwen Tang,<sup>a</sup> Andreas Kourtellaris,<sup>b</sup> Anastasios J. Tasiopoulos,<sup>b</sup> Simon J. Teat,<sup>c</sup>  
David Dubbeldam,<sup>a</sup> Gadi Rothenberg,<sup>a</sup> Stefania Tanase<sup>\*a</sup>

- a. Van 't Hoff Institute for Molecular Sciences, University of Amsterdam,  
Science Park 904, 1098 XH Amsterdam, The Netherlands.
- b. Department of Chemistry, University of Cyprus, 1678 Nicosia, Cyprus.
- c. Advanced Light Source, Lawrence Berkeley National Laboratory,  
Berkeley, California 94720, USA.

\*To whom correspondence should be addressed.

E-mail: [s.grecea@uva.nl](mailto:s.grecea@uva.nl)

## S1 Scheme of H<sub>4</sub>L Ligand



Scheme S1. Schematic representation of the H<sub>4</sub>L ligand structure.

## S2 X-ray Structure Analysis

Table S1. Crystal Data and Refinement Information for Complexes.

| Complexes                                | 1  | 2  | 3  | 4  |
|--|--|--|--|--|
| Formula                                  | C <sub>41</sub> H <sub>42</sub> Mg <sub>2</sub> N <sub>2</sub> O <sub>15</sub> | C <sub>78</sub> H <sub>75</sub> Ca <sub>4</sub> N <sub>3</sub> O <sub>27</sub> | C <sub>86</sub> H <sub>97</sub> Ca <sub>4</sub> N <sub>5</sub> O <sub>31</sub> | C <sub>84</sub> H <sub>84</sub> Sr <sub>4</sub> N <sub>6</sub> O <sub>30</sub> |
| Formula weight                           | 851.38   | 1646.73  | 1857.00  | 2008.05  |
| Space group                              | P <sub>bca</sub>   | P <sub>bca</sub>   | C222 <sub>1</sub>  | P-1  |
| a (Å)                                    | 12.5932 (2)  | 22.398 (2)   | 11.1690 (6)  | 14.287 (5)   |
| b (Å)                                    | 18.4157 (4)  | 30.468 (2)   | 24.2978 (13)   | 19.257 (5)   |
| c (Å)                                    | 33.2641 (6)  | 26.820 (2)   | 33.4201 (18)   | 19.522 (5)   |
| α (°)                                    | 90   | 90   | 90   | 65.213 (5)   |
| β (°)                                    | 90   | 90   | 90   | 73.212 (5)   |
| γ (°)                                    | 90   | 90   | 90   | 75.976 (5)   |
| Volume (Å <sup>3</sup> )                 | 7714.4 (2)   | 18303 (2)  | 9069.6 (8)   | 4623 (2)   |
| Z  | 8  | 8  | 4  | 2  |
| Dx (g/cm <sup>3</sup> )                  | 1.466  | 1.195  | 1.360  | 1.447  |
| μ (mm <sup>-1</sup> )                    | 1.228  | 2.666  | 0.402  | 2.376  |
| Reflections Collected                    | 28310  | 41341  | 64501  | 31939  |
| Reflections Unique                       | 6881   | 16258  | 10562  | 16259  |
| R <sub>1</sub> <sup>a</sup> [I > 2σ (I)] | 0.0568   | 0.0952   | 0.0459   | 0.0505   |
| wR <sub>2</sub> <sup>b</sup>             | 0.1603   | 0.2932   | 0.1222   | 0.1414   |

<sup>a</sup>R<sub>1</sub> = Σ||Fo| - |Fc|| / Σ|Fo|, <sup>b</sup>wR<sub>2</sub> = {Σ[w(|Fo|<sup>2</sup> - |Fc|<sup>2</sup>)<sup>2</sup>] / Σ[w(|Fo|<sup>4</sup>)]}<sup>1/2</sup>

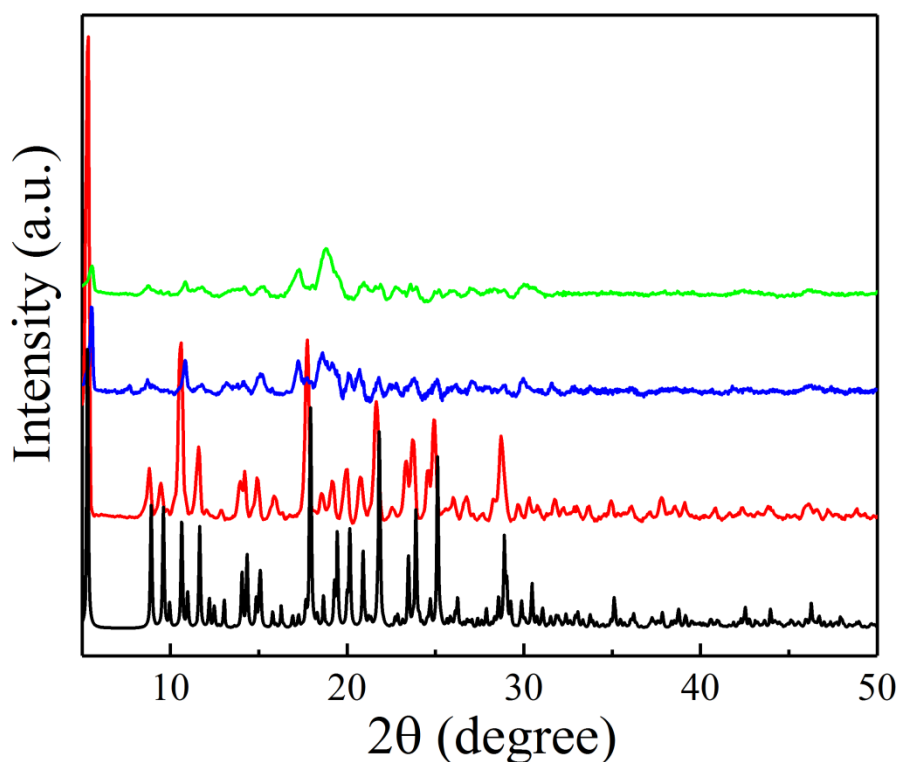


Fig. S1 PXRD patterns of the simulated **1** (black), as-synthesized **1** (red), activated **1** (blue) and compound **1** exposed at 98% relative humidity after 12h (green), respectively.

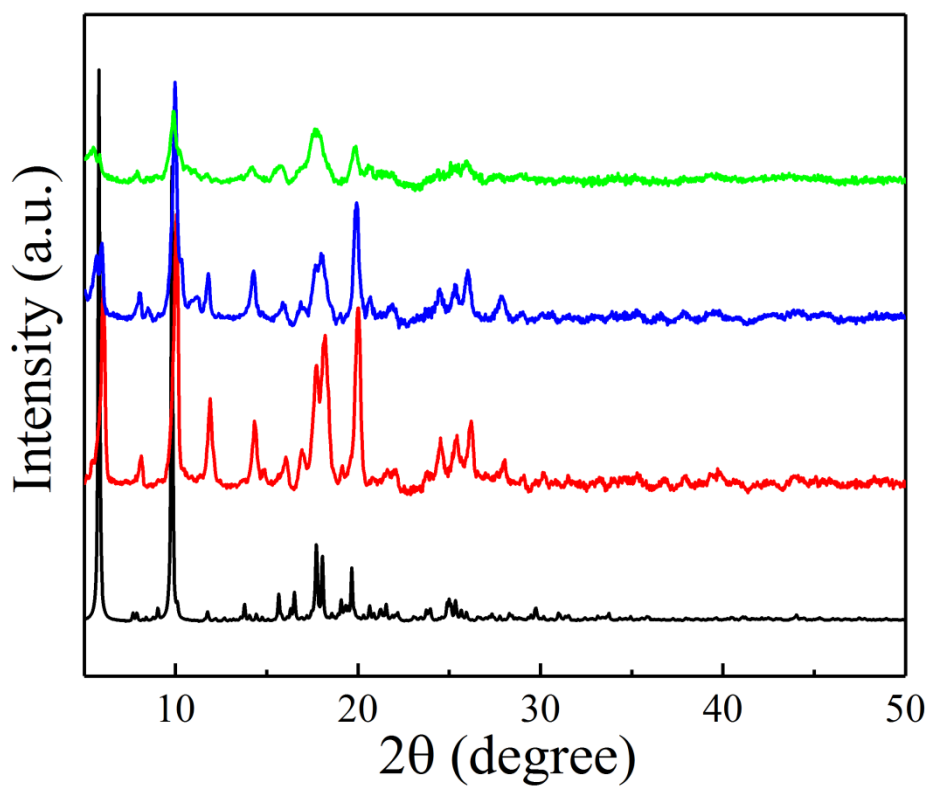


Fig. S2 PXRD patterns of the simulated **2** (black), as-synthesized **2** (red), activated **2** (blue) and compound **2** exposed at 98% relative humidity after 96h (green), respectively.

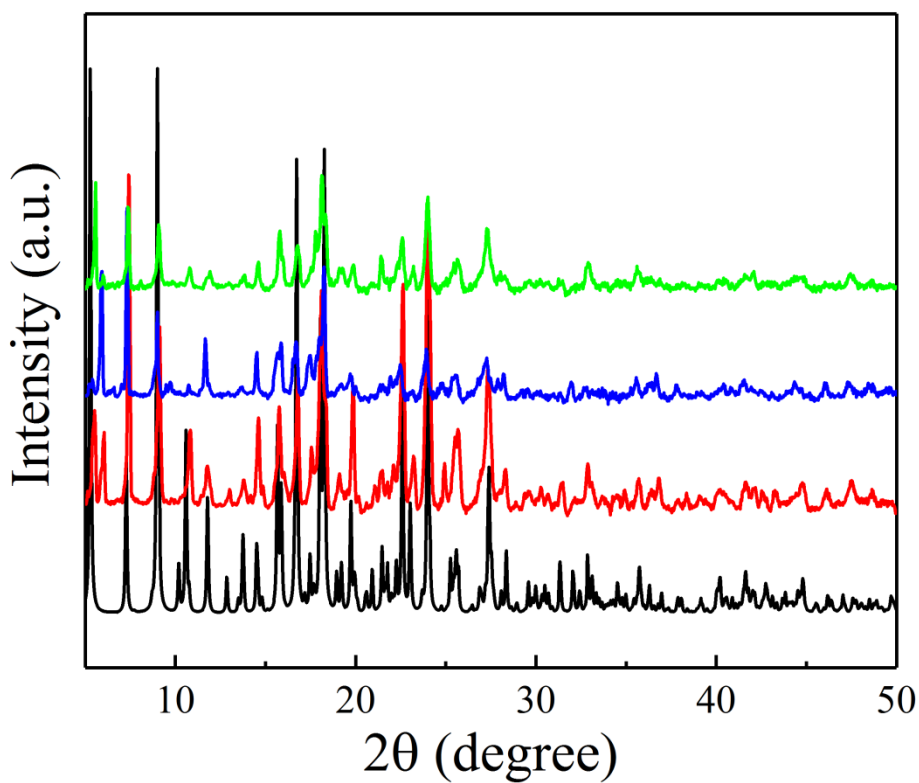


Fig. S3 PXRD patterns of the simulated **3** (black), as-synthesized **3** (red), activated **3** (blue) and compound **3** exposed at 98% relative humidity after 96h (green), respectively.

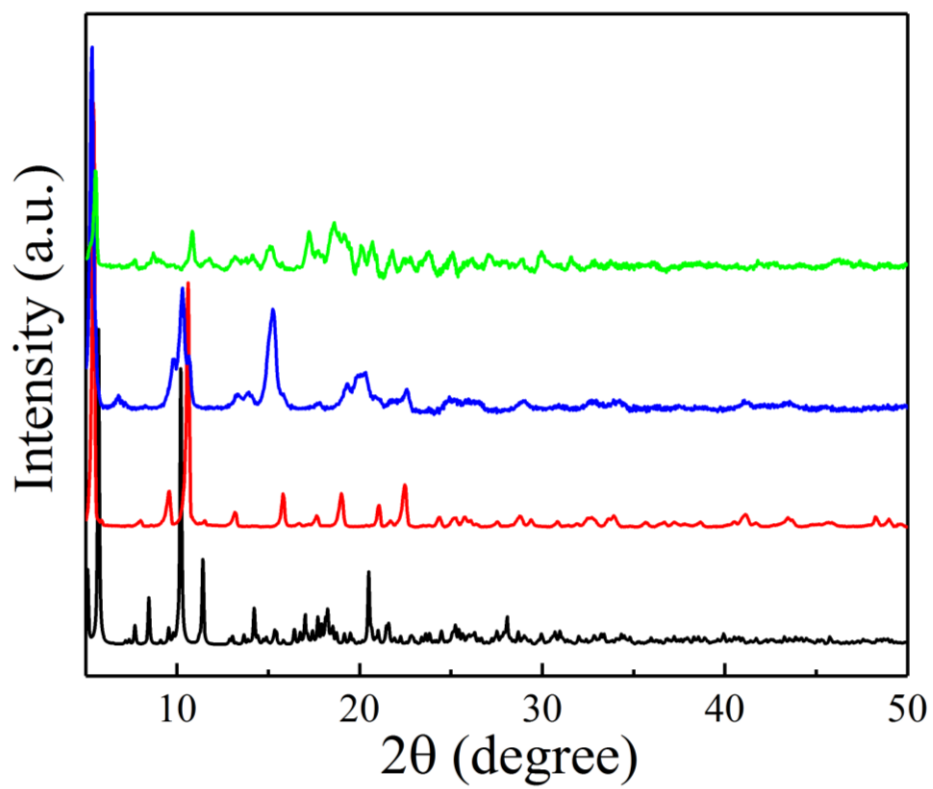


Fig. S4 PXRD patterns of the simulated **4** (black), as-synthesized **4** (red), activated **4** (blue) and compound **4** exposed at 98% relative humidity after 12h (green), respectively.

### S3 Thermal Stability

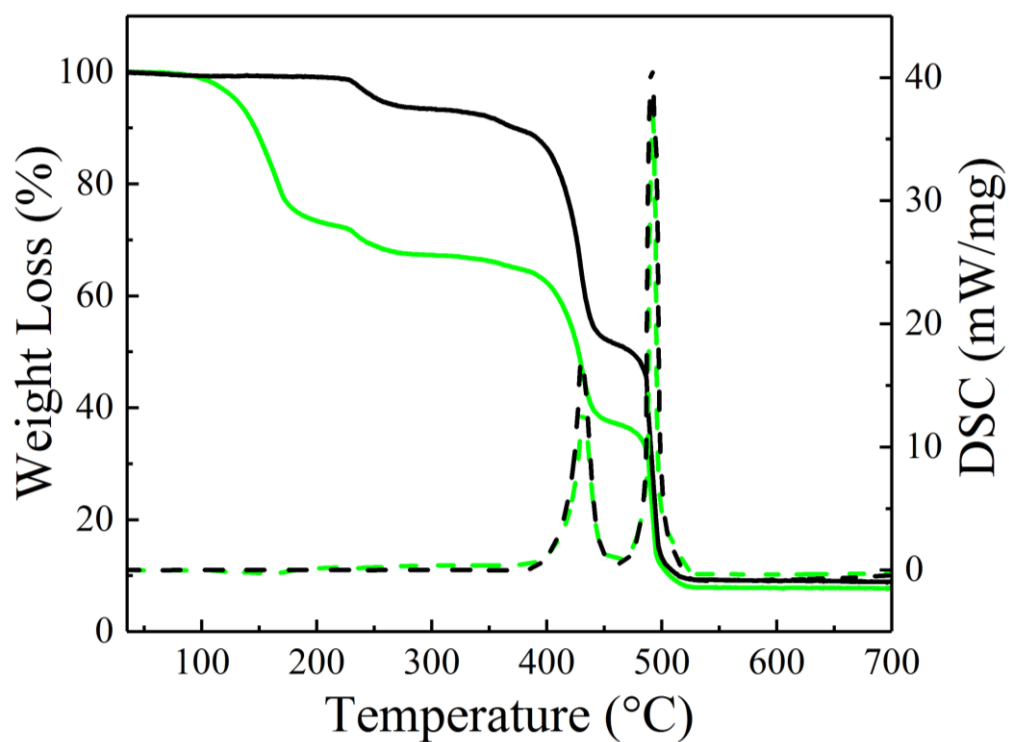


Fig. S5 TGA (solid line) and DSC (dash line) analysis of the as-synthesized **1** (green) and the activated **1** (black).

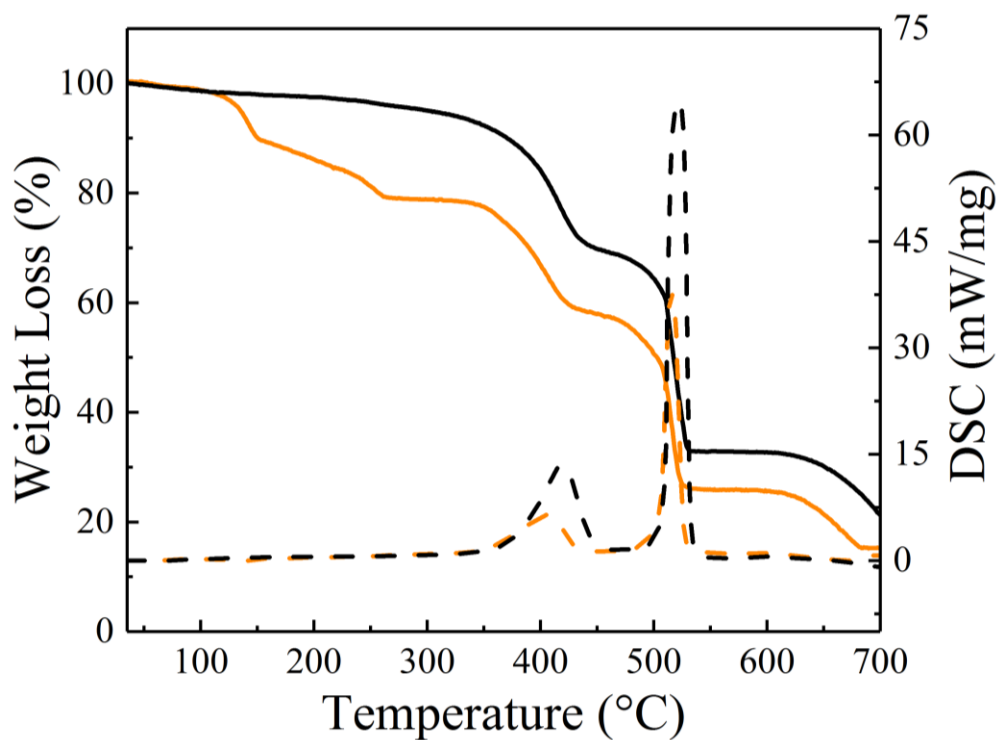


Fig. S6 TGA (solid line) and DSC (dash line) analysis of the as-synthesized **2** (orange) and the activated **2** (black).

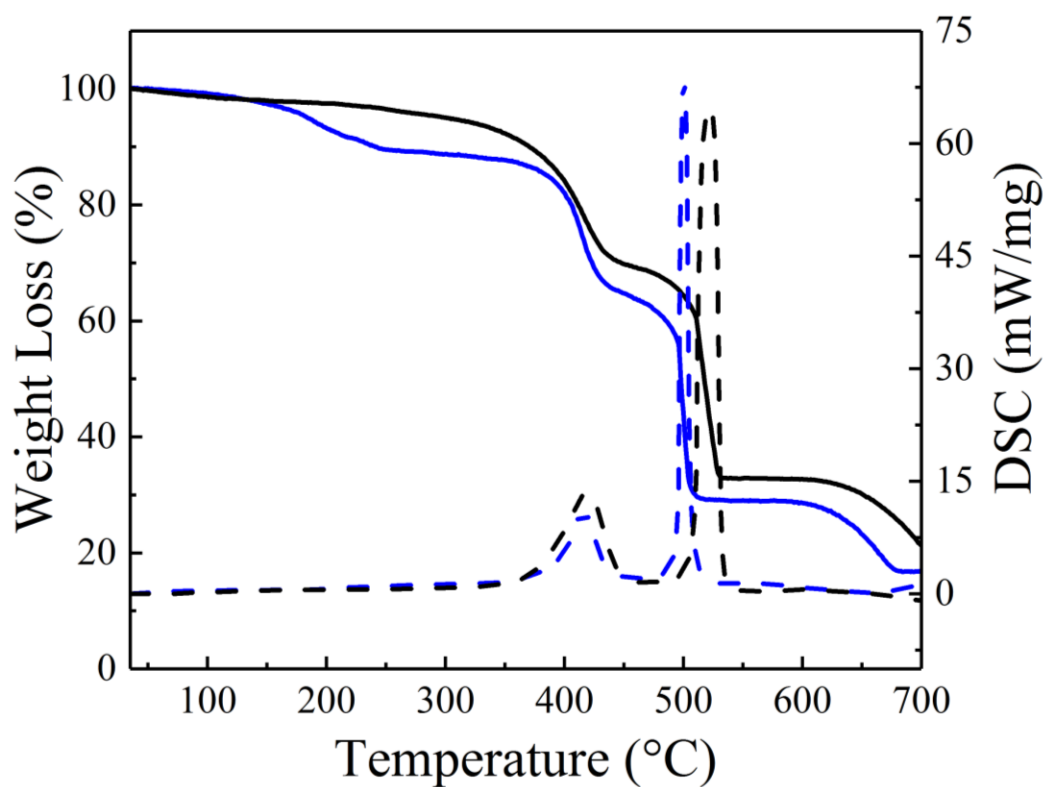


Fig. S7 TGA (solid line) and DSC (dash line) analysis of the as-synthesized **3** (blue) and the activated **3** (black).

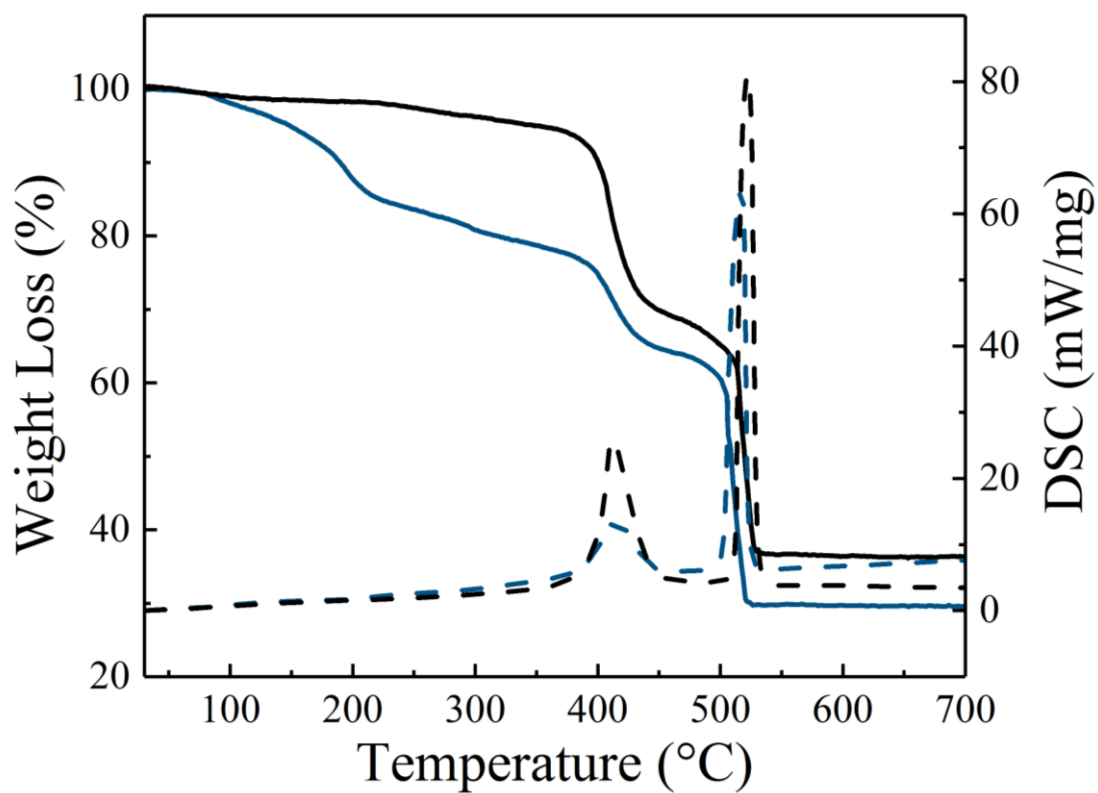


Fig. S8 TGA (solid line) and DSC (dash line) analysis of the as-synthesized **4** (dark blue) and the activated **4** (black).

**Table S2. Elemental Analysis of the Activated Alkaline-Earth Based MOFs**

|            | <b>1</b> | <b>2</b> | <b>3</b> | <b>4</b> |
|------------|----------|----------|----------|----------|
| C% (calc.) | 59.75    | 57.06    | 55.63    | 50.21    |
| C% (exp.)  | 58.24    | 57.60    | 55.45    | 49.66    |
| N% (calc.) | 1.00     | 0.95     | 1.75     | 0.85     |
| N% (exp.)  | 1.24     | 0.52     | 1.29     | 1.07     |
| H% (calc.) | 3.77     | 3.87     | 4.38     | 3.33     |
| H% (exp.)  | 4.72     | 4.21     | 3.92     | 3.76     |



## S4 Gas Adsorption

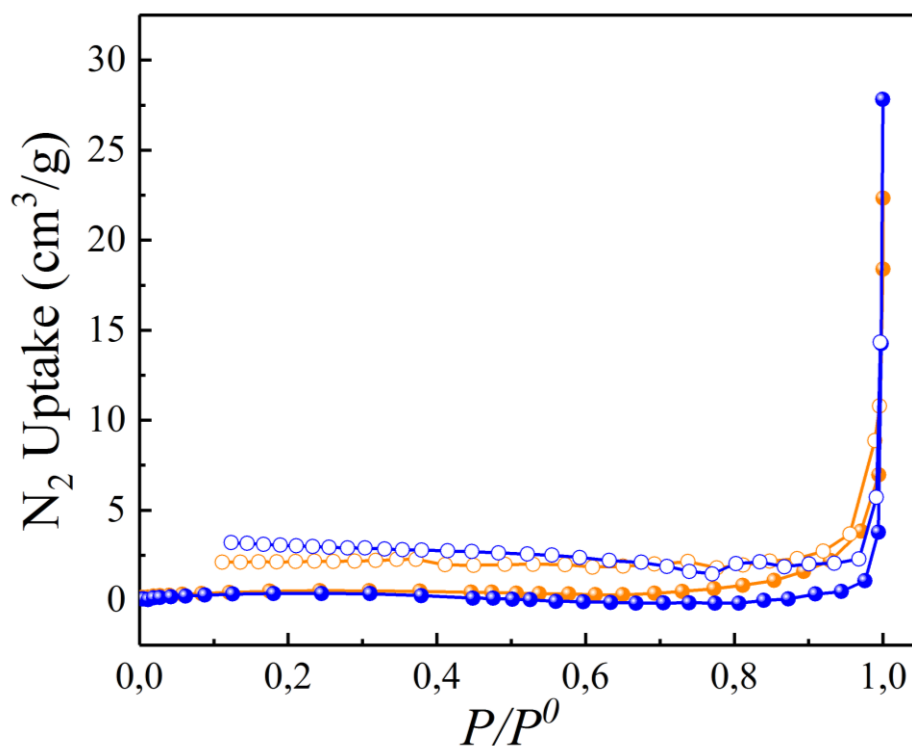


Fig. S9 N<sub>2</sub> uptake of the alkaline-earth metal-based MOFs **2** (orange) and **3** (blue) at 77 K. (Closed symbols correspond to the adsorption and the open symbols to the desorption). Adsorption isotherms of compounds **1** and **4** are not shown here for clarity and both of them do not show the N<sub>2</sub> uptake at 77 K.

## S5 IAST Adsorption Selectivity Calculation

IAST (ideal adsorption solution theory) is applied to predict mixed-gas adsorption isotherms from single-component adsorption isotherms.<sup>1,2</sup>

The experimental CO<sub>2</sub> adsorption isotherm data measured at 273 K for compounds **2** and **3** are fitted well with the BET equation:

$$n_i^o(P) = M \frac{K_A P}{(1 - K_B P)(1 - K_B P + K_A P)}$$

Here, P is the pressure of the bulk gas equilibrium with the adsorbed phase (bar), M is the adsorbed amount per mass of adsorbent (mol/kg; M=39.252 and 24.066 for compounds **2** and **3**, respectively), K<sub>A</sub> is the Langmuir constant for the first layer of the adsorbate molecules in direct contact with the surface, and K<sub>B</sub> is the constant for the second and higher layers of adsorbate molecules (K<sub>A</sub>=2.330 and 3.165 for **2** and **3**; K<sub>B</sub>=0.336 and 0.281 for **2** and **3**, respectively). The fitted data are then applied to predict binary CO<sub>2</sub>/N<sub>2</sub> adsorption with IAST.

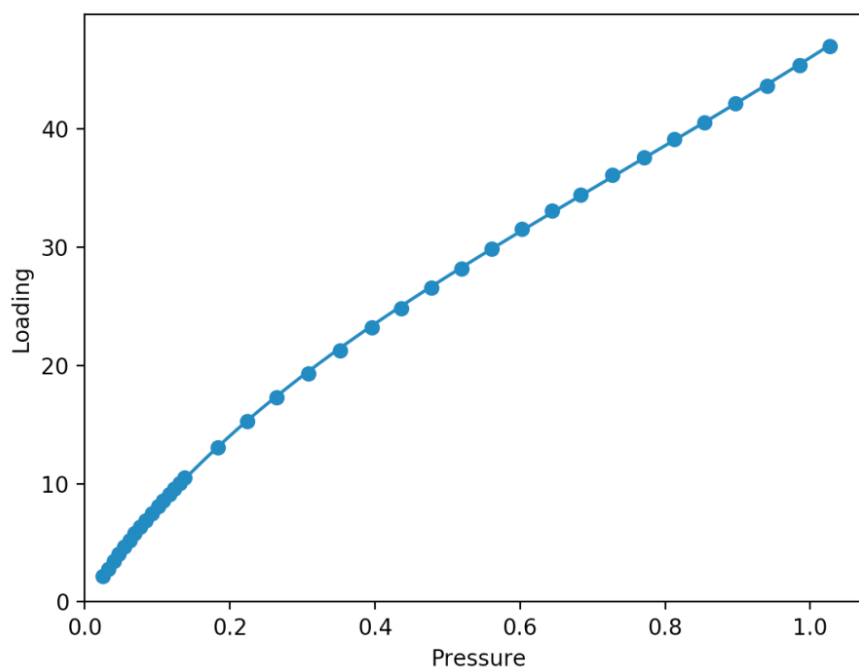


Fig. S10 CO<sub>2</sub> adsorption isotherm of compound **2** along with the BET model fit (Unit: Pressure in bar; Loading in cm<sup>3</sup>·g<sup>-1</sup>).

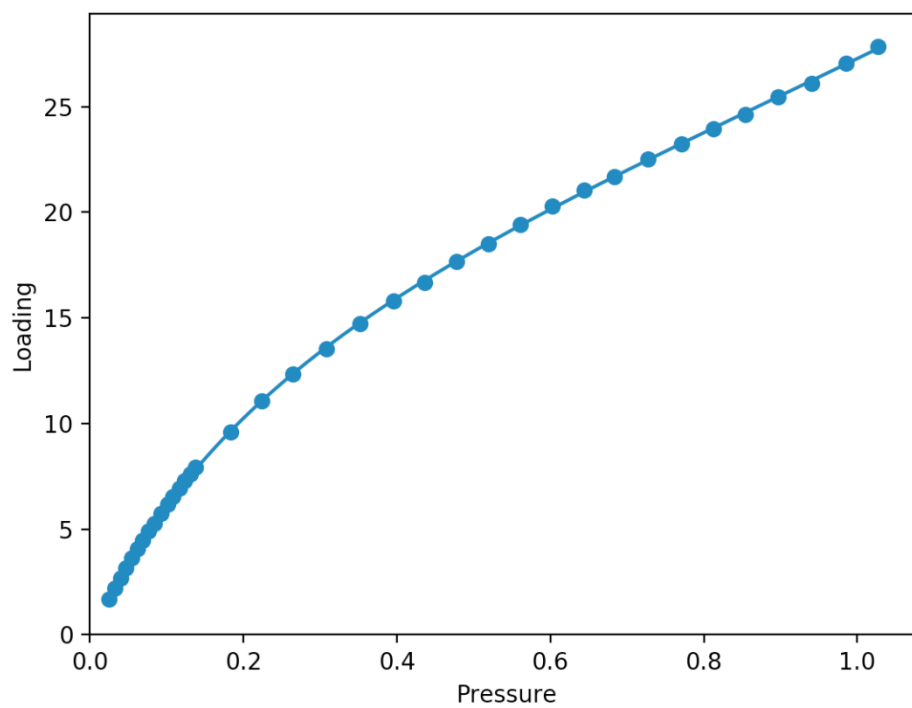


Fig. S11 CO<sub>2</sub> adsorption isotherm of compound **3** along with the BET model fit (Unit: Pressure in bar; Loading in cm<sup>3</sup>·g<sup>-1</sup>).

The experimental N<sub>2</sub> adsorption isotherm data measured at 273 K for compound **2** is fitted well with the *Henry's law* equation:

$$n_i^o(P) = K_H P$$

Here, P is the pressure of the bulk gas equilibrium with the adsorbed phase (bar), K<sub>H</sub> is the Henry coefficient (K<sub>H</sub>=2.241). The fitted data are then applied to predict binary CO<sub>2</sub>/N<sub>2</sub> adsorption with IAST.

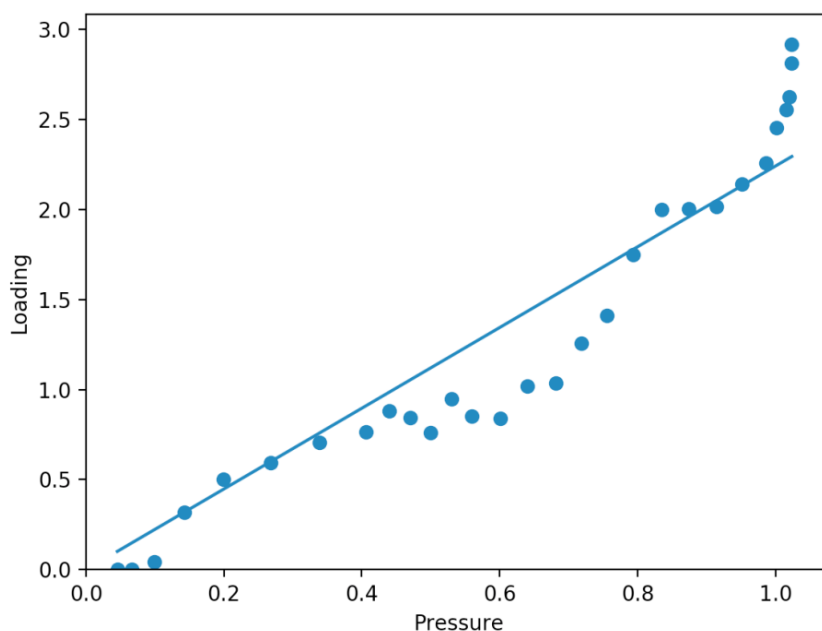


Fig. S12 N<sub>2</sub> adsorption isotherm of compound **2** along with the *Henry's law* model fit (Unit: Pressure in bar; Loading in cm<sup>3</sup>.g<sup>-1</sup>).

The experimental N<sub>2</sub> adsorption isotherm data measured at 273 K for compound **3** is hard to fit any models within IAST method, so we choose the numerical interpolation for this one and added an artificial point 10.0, 16.0 and 16.0 after that for all pressures. The fitted data are then applied to predict binary CO<sub>2</sub>/N<sub>2</sub> adsorption with IAST.

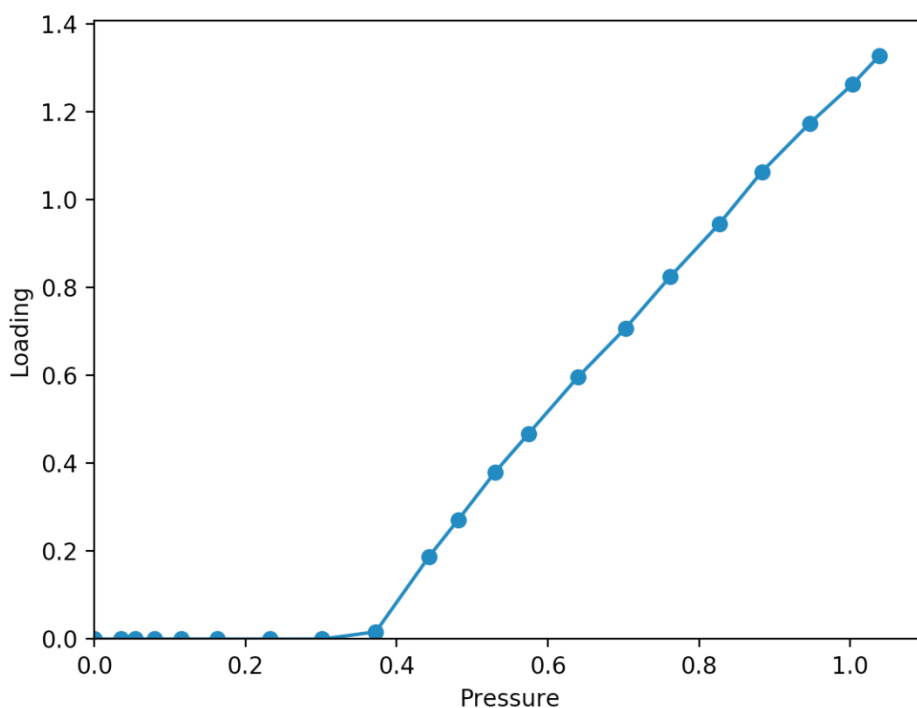


Fig. S13 N<sub>2</sub> adsorption isotherm of compound **3** along with the numerical interpolation method (Unit: Pressure in bar; Loading in cm<sup>3</sup>·g<sup>-1</sup>).

The adsorption selectivity of CO<sub>2</sub> over N<sub>2</sub> in a binary mixture is defined as:

$$S_{CO_2/N_2} = \frac{x_{CO_2}/y_{CO_2}}{x_{N_2}/y_{N_2}}$$

Here,  $x$  and  $y$  are the mole fractions of CO<sub>2</sub> and N<sub>2</sub> in the adsorbed and gas phases, respectively.

## References

- [1] A. L. Myers and J. M. Prausnitz, *AIChE. J.*, **1965**, 11, 121-127.
- [2] C. Simon, B. Smit, M. Haranczyk. (2016) pyIAST: Ideal Adsorbed Solution Theory (IAST) Python Package. *Computer Physics Communications*. 200, pp.364-380.